Journal of the Energy Institute 89 (2016) 101–114

Contents lists available at ScienceDirect

Journal of the Energy Institute

journal homepage: http://www.journals.elsevier.com/journal-of-the-energy-institute

Knock onset prediction of propane, gasoline and their mixtures in spark ignition engines

Stefano Beccari*, Emiliano Pipitone, Giuseppe Genchi

University of Palermo, Italy

ARTICLE INFO

Article history:
Received 31 July 2014
Received in revised form
31 December 2014
Accepted 11 January 2015
Available online 29 January 2015

Keywords:
Spark ignition engine
Knock onset
Propane
LPG
Modelling

ABSTRACT

Gaseous fuels, such as Liquefied Petroleum Gas (LPG) and Natural Gas (NG), thanks to their excellent mixing capabilities and high knocking resistance, allow complete and cleaner combustion than gasoline in Spark Ignition (SI) engines, resulting in lower pollutant emissions, above all if particulate matter is considered. In previous works [1,2] the authors proved how the simultaneous combustion of gasoline and gaseous fuel (NG or LPG) may strongly reduce both fuel consumption and pollutant emissions with respect to pure gasoline operation without a significant power loss. These very encouraging results were obtained thanks to the strong knock resistance increase obtained adding gaseous fuel to gasoline, which allowed the use of stoichiometric mixtures and better spark advances, even at full load. The introduction of such a kind of combustion in series production engines would however require the use of properly calibrated simulation models, capable to adequately predict the performance and efficiency of engines fuelled by gaseous fuel-gasoline mixtures; in particular, specific combustion models are needed, together with reliable knock onset prediction sub-model. The total absence of such sub-models in the scientific literature induced the authors to investigate the knocking resistance of gasoline-propane mixtures and calibrate a proper knock onset prediction sub-model to be implemented in the zero dimensional thermodynamic models usually employed for engine performance optimization. To this purpose several light knocking in-cylinder pressure cycles have been recorded on a CFR engine, fuelled by gasoline, propane and their mixtures, varying the most important knock-related parameters: compression ratio, spark advance, inlet mixture temperature and fuel mixture composition. The collected data have been used to calibrate two different models, compared in terms of knock onset prediction accuracy: the Knock Integral model (KI) and the Ignition Delay model (ID). Both models revealed a good reliability in predicting the onset of knocking phenomena, with maximum errors around 4 crank angle degrees. The Knock Integral model showed a slightly higher accuracy, which, together with its lower computational effort, makes it preferable for the implementation in the commonly employed thermodynamic engine models.

1. Introduction

In the last decades the automotive industry has concentrated many research efforts on alternative fuels. As regards Spark Ignition (SI) engines, gaseous fuels, such as Liquefied Petroleum Gas (LPG) and Natural Gas (NG), proved to be valid alternatives to gasoline. Nowadays a wide variety of bi-fuel engines already went into series production: these engines, endowed of two separate injection systems, may run using either gasoline or gas (NG or LPG). Since usually designed for gasoline operation, these engines however do not fully exploit the higher knocking resistance of gaseous fuel which would allow higher volumetric compression ratios and hence higher thermodynamic efficiency. As is known, at high engine loads, gasoline fuelled SI engines usually require rich fuel-air mixtures and retarded combustion phase to avoid knocking, thus generating high specific fuel consumption and pollutant emissions. Gaseous fuels instead, thanks to their higher auto-ignition temperature, allow the engine to run with stoichiometric air-fuel mixture even at full load, thus obtaining higher engine efficiency and lower pollutant emissions. Unfortunately, due to their low density, gaseous fuels reduce the engine power output with respect to

* Corresponding author.
E-mail address: stefano.beccari@unipa.it (S. Beccari).

http://dx.doi.org/10.1016/j.joei.2015.01.006
1743-9671/

gasoline. In previous works the authors showed that the simultaneous combustion of gasoline and gas (LPG [1] or NG [2]) in a SI engine, called *Double-Fuel* combustion, allows to exploit the best qualities of both fuels: this means to obtain the low specific fuel consumption and pollutant emissions of gas together with nearly the same power output of gasoline. The addition of gas to the gasoline increases the overall knock resistance which in turns allows the engine to run with overall stoichiometric air-fuel ratio and better spark advance. The simultaneous combustion of gas and gasoline has been successively investigated also by other researchers [3–6], both in naturally aspirated and supercharged SI engines. The results always showed strong engine efficiency increase and pollutant emissions reduction with respect to pure gasoline operation. The simultaneous combustion of gasoline and gas could be easily implemented in current production bi-fuel engines simply re-programming the electronic control unit; in particular, the Double-Fuel injection time and spark advance maps should be predetermined by proper calibration tests and added to the ECU memory. This calibration process may however require a huge amount of experimental tests. Computer simulations represent a fundamental step in the design and performance optimization phase; zero dimensional models of the in-cylinder transformations coupled to 1-dimensional models of the intake and exhaust ducts flows are nowadays widely spread in the automotive industry as effective tool for engine performance optimization, allowing a fast and reliable determination of injection time and spark advance maps, thus strongly reducing the amount of experimental tests to carry out. However, since knocking is a crucial issue concerning SI engines, a reliable knock onset prediction sub-model, specific for Double-Fuel operation, should be employed so as to safely maximize engine efficiency. The sub-model should predict knock occurrence with acceptable accuracy for each proportion between gasoline and gaseous fuel. Several knock prediction models have been used to test both gasoline and gaseous fuels [7–12,14,15] but only a few of them deal with mixtures composed by gasoline and gaseous fuel [13,21,28]. Considering the lack of literature on this argument and the significant potential of this kind of fuel mixtures in SI engines future development, the authors decided to investigate the knock resistance of gasoline-propane fuel mixtures in different proportions. Engine development and optimization process usually involves numerical simulations and experimental tests performed using reference fuels, whose known properties allow to trace repeatable and comparable results. Therefore in this work the propane has been used in place of the most common and commercially available LPG whose properties, first of all its knock resistance, strongly depends on its chemical composition [21,34], which may also vary according to the production site and season.

The knock onset prediction sub-models mostly employed for engine development can be grouped in two main categories: ignition delay models and detailed chemical kinetic models. Both kinds of model are designed for zero dimensional simulations, being the unburned gas pressure and temperature represented in terms of mean values over the whole end-gas mass. The models of the first category base their prediction on the unburned gas pressure and temperature histories and usually need some experimental data for the tuning of their parameters [7–13]. Chemical kinetic models, instead, take into account the elementary reaction steps that occur between the chemical species involved in the combustion process [16,17]. Unfortunately, due to the complex fuel composition, some of the elementary reactions may be unknown; moreover, due to the high number of reactions to consider, chemical kinetic sub-models always require a great computational effort. For these reasons the first category is often preferred for the estimation of unburned gas auto-ignition time. The models based on ignition delay originates with experiments carried out in rapid compression machines [7], where the compression, produced by a very rapid stroke, allows to estimate the fuel auto-ignition delay for a given constant pressure and temperature condition. The ignition delay τ [s], defined as the time between the end of the rapid compression and the auto-ignition, can be hence correlated with the constant fuel-air mixture pressure p [bar] and temperature T [K] by means of an Arrhenius type equation:

$$\tau = A \cdot p^{-n} \cdot e^{E/R \cdot T} \tag{1}$$

where E [J/mol] is the fuel activation energy, R [J/mol K] is the universal gas constant, A and n are fuel dependent parameters, which can be tuned by means of experimental data. Since in SI engines the unburned gas pressure and temperature are not constant, the above correlation is employed with two different approaches: the Livengood and Wu Knock Integral approach [7,9–13,18,19] and the Ignition Delay approach [8]. The first is based on the evaluation of the following Knock Integral (KI):

$$KI(t) = \int_{t_{IVC}}^{t} \frac{dt}{\tau} = \int_{t_{IVC}}^{t} \frac{dt}{A \cdot p^{-n} \cdot e^{B/T}} \tag{2}$$

where t_{IVC} is the inlet valve closure time, while the parameter B substitutes the ratio E/R. According to this method, the knock onset time t_{KO} is obtained when the integral reaches the value of 1:

$$\boldsymbol{KI(t_{KO}) = \int_{t_{IVC}}^{t_{KO}} \frac{dt}{A \cdot p^{-n} \cdot e^{B/T}} = 1} \tag{3}$$

this condition corresponds to the critical concentration of the radical species needed for the auto-ignition. The second method, instead, evaluates the Ignition Delay (ID) with respect to spark time by means of the unburned gas mean pressure p_m and temperature T_m, both estimated during the whole combustion period:

$$ID = A \cdot p_m^{-n} \cdot e^{B/T_m} \tag{4}$$

With the aim to obtain a reliable knock prediction sub-model for gasoline-propane fuel mixtures, the KI method of Equations (2) and (3) and the ID method of Equation (4) have been separately calibrated by means of a large amount of experimental data and then compared in terms of knock onset prediction accuracy. Both methods are well known and widely applied in current zero dimensional models for in-cylinder thermodynamic simulations: the calibration results here proposed hence allow to extend their field of application to fuel mixtures composed by gasoline and propane in different proportions. Since the methods are based on the unburned gas pressure and temperature history, the authors decided to tune the models parameters by means of experimental data characterized by a significant variation

of these two thermodynamic quantities. This comprehensive calibration process gives the model a general validity, making it suitable for predicting knock occurrence in SI engines of different kind, for example naturally aspirated or supercharged, and for various proportions between the two fuels in the propane-gasoline mixture. The experimental campaign has been carried out by means of a CFR engine, which, thanks to its particular arrangement, allowed great variations of volumetric compression ratio and inlet mixture temperature, thus obtaining a widely diversified set of pressure and temperature histories. The tuned knock prediction models can be easily implemented in usual zero dimensional numerical simulations involving the same fuel mixture and different engines since the tuned parameters depend only on fuel type [10], while the engine is responsible for the pressure and temperature histories.

2. Experimental setup and test method

The experimental campaign of the present work has been carried out using a Cooperative Fuel Research (CFR) engine [20] manufactured by Dresser Waukesha, whose main specifications are resumed in Table 1.

The CFR engine is a four-stroke two valve stationary single-cylinder spark-ignition engine. The particular engine arrangement allows to vary quickly and accurately the Compression Ratio (CR) from 4.5 to 16 by moving the engine head (fixed to the cylinder sleeve) with respect to the crankshaft. The combustion chamber is of discoid type and its basic configuration does not change with the compression ratio. The CFR engine is connected to an electric synchronous motor that maintains a constant speed of 900 rpm both in fired and motored condition. The engine is equipped with an electronically controlled inductive discharge ignition system and with a two electric heaters which have been connected to two independent PID control systems Omega CN4116 in order to maintain both inlet air temperature and air/fuel mixture temperature at the required values during the tests. The CFR is also equipped with a thermo siphon cooling system to maintain the cylinder jacket coolant temperature at 100 ± 1.5 °C. All the temperatures were measured using K-type thermocouples. As regards fuel supply, a standard CFR engine features an original carburettor system which does not allow the use of gaseous fuels. The authors hence endowed the CFR engine with two independent injection systems in order to run either with gasoline or with propane and to accurately control the air-fuel ratio. To this purpose, a Venturi type air mass flow meter was employed, while the two Bosch port fuel injectors were placed on the CFR intake duct (Fig. 1), before the carburettor that was not used in the tests.

As shown in Fig. 1, the gaseous fuel stored in a reservoir tank passes through a Bronkhorst mini CORI-FLOW® Coriolis effect mass flow meter (with a 0.1–2.0 kg/h measurement range and the accuracy of ±0.2% of reading value) and hence through a pressure regulator, used to maintain the injector feed pressure of 3 bar. The gasoline injection system instead is composed by an electric fuel pump, an automatic pressure regulator used to maintain a constant injection pressure of 4 bar, a fuel cooler placed on the return line to ensure a proper gasoline temperature, and the gasoline port injector. During the tests, the gasoline mass flow was deduced on the base of the imposed injection time by means of a proper injector flow chart previously determined [21]. A personal computer was used to manage the two injection systems and perform data acquisition, by means of an expressly designed software developed by the authors in LabVIEW environment. A properly developed [21] electrical circuit has been employed for the activation of each fuel injector, mainly composed by the power supply, the injector solenoid and transistors specifically designed for automotive injection/ignition application [21,22].

A National Instruments DAQCard 6062E programmed in LabVIEW environment has been used to generate the injection digital pulses, whose high level duration is exactly the injection time: the modulation of this high level width allowed hence the precise control of the amount of fuel injected. The injection times of the two fuels were modulated following two different strategies: propane injection was controlled in closed-loop using as feedback the overall air-to-fuel ratio, calculated on the basis of both fuels and inlet air mass flow rates. Gasoline injection, instead, was operated in open-loop, pursuing the predetermined proportion between the two fuels. All the relevant quantities (intake duct pressure, propane and inlet air mass flows, inlet air and air-fuel mixture temperatures) were acquired by means of the mentioned National Instruments DAQCard 6062E using as trigger the pulse generated by an incremental optical encoder connected to the engine crankshaft. The same trigger has been employed to synchronize the injection digital pulses with the piston movement. The knock occurrence was monitored using a Kistler piezoelectric pressure sensor, flush mounted on the combustion chamber. A second personal computer was used to process the in-cylinder pressure signal acquired with 120 kHz sampling frequency by means of a second National Instruments DAQCard 6062E and using the encoder single pulse per revolution to trigger the acquisition (Fig. 1). The intake duct pressure was measured by means of a DRUCK piezoresistive pressure sensor and has been employed to compensate the acquired pressure cycles [20,24]. A fundamental aspect in indicating analysis is the precise determination of the Top Dead Centre (TDC) position [25,26] which has been accomplished by the use of a Kistler capacitive sensor 2629B, characterized by a 0.1 Crank Angle Degrees (CAD) accuracy. In order to differentiate as much as possible the pressure and temperature histories of the unburned gas, the experimental campaign has been designed fixing, for each fuel mixture, the spark advance and the inlet temperature and increasing the engine compression ratio until light knocking occurrence; this procedure has been performed for three spark advances, namely 15, 25 and 35 CAD before TDC, and four inlet mixture temperatures, namely 50, 80, 110 and 140 °C; the spark advances have been fixed to avoid combustion ignition onset too different from that of actual engines. As reported in Table 2, the experimental tests have been carried out with gasoline, propane and their mixtures. The composition of propane-gasoline mixtures was changed from 20% to 80% of propane mass fraction x_{prop} (i.e. the percentage mass of propane

Table 1
CFR Engine Specifications [20].

Manufacturer	Dresser waukesha
Model	F1/F2 Octane
Compression ratio	4.5–16
Bore	82.6 [mm]
Stroke	114.3 [mm]
Connecting rod length	254.0 [mm]
Displacement	611.2 [cm^3]
Speed	900 [rpm]

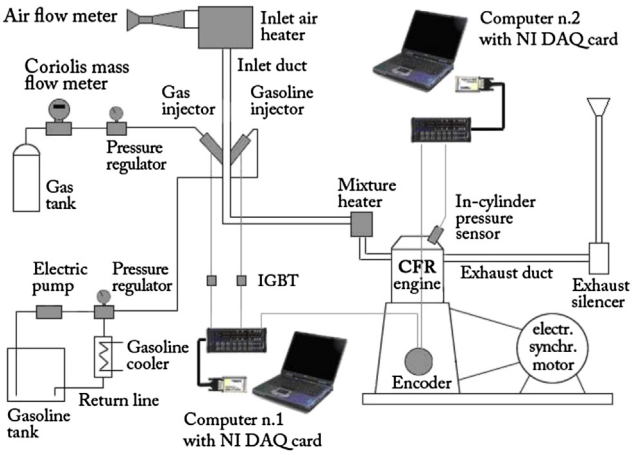

Fig. 1. Experimental system layout.

in the total fuel mass of the mixture). The overall air-fuel ratio was always maintained stoichiometric because, as previously shown for Double-Fuel operation mode [1,2], this produces the best results in terms of both engine efficiency and pollutant emissions. For each of the 72 operative conditions tested (resumed in Table 2) 50 consecutive knocking cycles were sampled. As a result of the wide variation of experimental condition, the in-cylinder peak pressure ranged from 22 to 42 bar while the end-gas peak temperature varied from 550 to 820 K: such a widely differentiated amount of pressure and temperature histories have been used for calibration with the aim to produce a knock onset prediction model valid for engines of different kind (i.e. aspirated and supercharged) and geometries (i.e. compression ratio).

Table 3 reports the compression ratios used in all the operative conditions tested, while the characteristics of the gasoline [30,38,39] and propane [34,40] used in the tests are resumed in Table 4.

Table 2
Test conditions.

Engine speed	900 [RPM]
Inlet temperature (T_{IN})	50, 80, 110, 140 [°C]
Engine load condition	Full load
Compression ratio values (light knocking)	From 5.66 to 9.04
Overall air/fuel ratio	Stoichiometric
Spark advance (SA)	15, 25, 35 [CAD BTDC]
Propane mass fraction	From 0% to 100% with step of 20%

Table 3
Engine compression ratios used in the tests.

SA BTDC [CAD]	T_{IN} [°C]	Propane mass fraction (%)					
		0	20	40	60	80	100
15	50	7.77	8.03	8.50	8.69	9.04	9.04
	80	7.34	7.67	7.82	8.09	8.38	8.38
	110	7.08	7.25	7.52	7.67	7.82	7.92
	140	6.81	6.88	7.16	7.29	7.43	7.52
25	50	6.73	6.88	7.16	7.29	7.57	7.52
	80	6.45	6.52	6.70	6.81	7.00	7.12
	110	6.23	6.23	6.39	6.45	6.62	6.81
	140	5.92	6.00	6.11	6.08	6.29	6.45
35	50	6.29	6.52	6.81	6.88	7.12	7.34
	80	6.00	6.20	6.36	6.56	6.73	6.92
	110	6.06	5.92	6.06	6.20	6.36	6.45
	140	5.74	5.66	5.74	5.86	6.00	6.29

Table 4
Gasoline and propane properties.

Properties	Gasoline	Propane
Composition	mixture of C_4–C_{12} hydrocarbon	≥99% C_3H_8
Molar mass [g/mole]	103–114	44
MON	85	96.7
Lower heating value [MJ/kg] [29]	43.4	46.3
Stoichiometric air-fuel ratio	14.7	15.7

The unburned gas temperature T was calculated, from Inlet Valve Closure (IVC) to spark ignition (SI) time, by means of the perfect gas law:

$$T = T_{IVC} \cdot \frac{p \cdot V}{p_{IVC} \cdot V_{IVC}} \tag{5}$$

where V is the in-cylinder volume, p is the gas pressure, p_{IVC}, V_{IVC} and T_{IVC} are the pressure, volume and temperature at IVC. The assumption at the basis of Equation (5) is the absence of gas leakage from the cylinder that is largely acceptable. The temperature T_{IVC} has been set equal to the inlet temperature T_{MIX} thus neglecting the in-cylinder heat transfer. Since starting of combustion, the burned and unburned gas temperatures differ from each other and the respective masses and volumes changes continuously: this make Equation (5) no more valid. Hence, following an assumption widely accepted when dealing with zero dimensional modelling of in-cylinder thermodynamics, after spark ignition, the unburned gas temperature T has been assumed to follow an isentropic law:

$$T = T_{IGN} \cdot \left(\frac{p}{p_{IGN}}\right)^{\frac{m-1}{m}} \tag{6}$$

where T_{IGN} and p_{IGN} are the unburned gas temperature and pressure at spark ignition time, while m is the isentropic coefficient, which, following the indication in [23,24] has been fixed to 1.32. The assumption at the basis of Equation (6) is that, during the combustion, the heat transferred by the end-gas to the cylinder walls is counterbalanced by the heat received from the flame front: the net heat flux is then null and the result is an isentropic evolution.

Fig. 2 shows an example of raw pressure signal power spectrum; the knocking pressure oscillations have a main frequency of about 6 kHz. The pressure signal has been filtered by means of a second order, zero-phase shift, band-pass 3–20 kHz Butterworth filter in order to remove unwanted noise and highlight knocking pressure oscillations. For each recorded pressure cycle, the experimental Knock Onset Crank Angle (KOCA) $\vartheta_{KO,exp.}$ has been identified as the location of the first band pass filtered pressure oscillation with a peak to peak value higher than 0.2 bar: this threshold has been fixed based on previous experimental observations. With the aim to obtain a model that correctly predicts the incipient knocking, the pressure cycles with peak to peak oscillations higher than 0.6 bar have been excluded from the calibration procedure. Fig. 3 shows a typical light knocking pressure curve, obtained with a 60% propane fuel mixture, together with its band-pass filtered signal: the $\vartheta_{KO,exp.}$ is highlighted.

Once determined the $\vartheta_{KO,exp.}$ for each of the pressure cycle sampled, the KOCA $\vartheta_{KO,est,INT}$ estimated by the integral model has been evaluated by solving the Knock Integral of Equation (3) in the crank angle domain until reaching the value of 1:

$$\int_{\vartheta_{IVC}}^{\vartheta_{KO,est,INT}} \frac{d\vartheta}{\omega \cdot A \cdot p^{-n} \cdot e^{B/T}} = 1 \tag{7}$$

where ϑ_{IVC} is the IVC crank angle and ω is the engine angular velocity [rad/s]. The KOCA error ε_{INT} can be evaluated for each fixed set of constants A, n, and B by means of the following equation:

$$\varepsilon_{INT} = \vartheta_{KO,est,INT} - \vartheta_{KO,exp.} \tag{8}$$

As regards the ID method, the estimated KOCA, according to Equation (4), is:

$$\vartheta_{KO,est,ID} = \omega \cdot A \cdot p_m^{-n} \cdot e^{B/T_m} \tag{9}$$

where p_m [bar] and T_m [K] are the unburned gas mean pressure and temperature evaluated during the combustion period [8] (i.e. starting from SI rather than IVC). The KOCA error ε_{ID} can be then evaluated as:

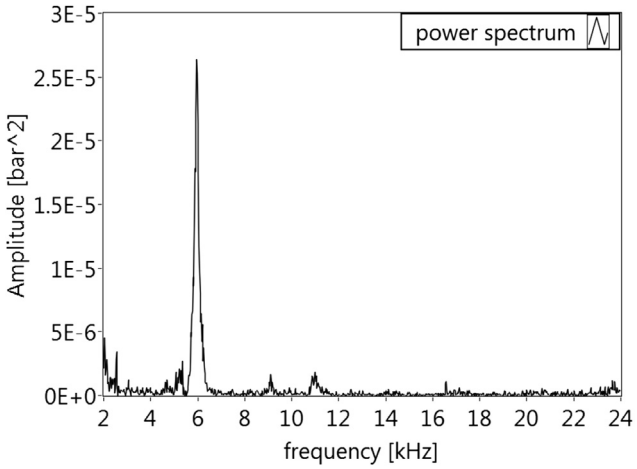

Fig. 2. Power spectrum of the raw pressure signal (60% propane – 40% gasoline, SA = 25 CAD BTDC, T_{MIX} = 50 °C).

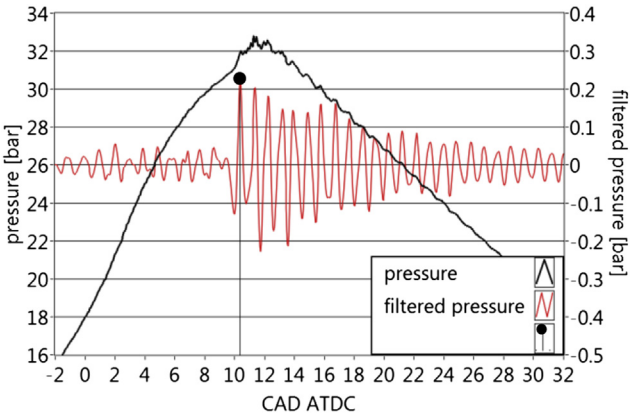

Fig. 3. Raw and filtered pressure with $\vartheta_{KO,exp.}$ evaluation, (60% propane − 40% gasoline, SA = 25 CAD BTDC, T_{MIX} = 50 °C).

$$\varepsilon_{ID} = \vartheta_{KO,est,ID} - \vartheta_{KO,exp.} \tag{10}$$

3. Experimental results and discussion

The Knock Integral model was initially calibrated using the pressure cycles obtained with gasoline and propane. The optimal set of model parameters *A, n* and *B* has been determined minimizing the mean absolute error $\varepsilon_{MA,INT}$ evaluated over the total number of pressure cycles *N*:

$$\varepsilon_{MA,\ INT} = \frac{\sum_{i=1}^{N} |\varepsilon_{INT,\ i}|}{N} \tag{11}$$

where $\varepsilon_{INT,\ i}$ is the KOCA error determined for the *i*th knocking pressure cycle. For fixed values of *n* and *B*, the parameter *A* has been varied using the Downhill Simplex searching algorithm [27] in order to minimize the objective function $\varepsilon_{MA,INT}$ *(A, B, n)*; this method has been repeated for *B* ranging from 1000 to 5500 and *n* ranging from 1.5 to 3.5: these ranges of variation have been fixed considering the mean values suggested in literature for gasoline [7,10,13] and propane [14,15]. The model has been tuned minimizing the KOCA error instead of integral error (i.e. the difference between the Knock Integral value at knock onset and 1) because the first better represents the model prediction accuracy for engine calibration purposes, since it represents the model error in terms of crank angle degrees. This procedure allowed to trace the surface and the contour map of the minimum $\varepsilon_{MA,INT}$ as function of *B* and *n*, which, as example, are reported in Fig. 4 and Fig. 5 respectively, for the gasoline case: the cross indicates the absolute minimum of $\varepsilon_{MA,INT}$ and allow to determine the best values of the three model parameters, reported in Table 5 together with the mean and the maximum absolute error. Table 5 also shows the values obtained for propane, which, as can be noted, are quite different from that of gasoline due to the different knock resistance of the two fuels; in particular the greater value of B determined for propane corresponds to its higher activation energy (see Equation (1)).

Almost the same procedure has been followed applying the Ignition Delay method (4). For each fixed set of model parameters *A, n* and *B* the KOCA error ε_{ID} has been evaluated by Equation (10) and the mean absolute error $\varepsilon_{MA,ID}$ by the following equation:

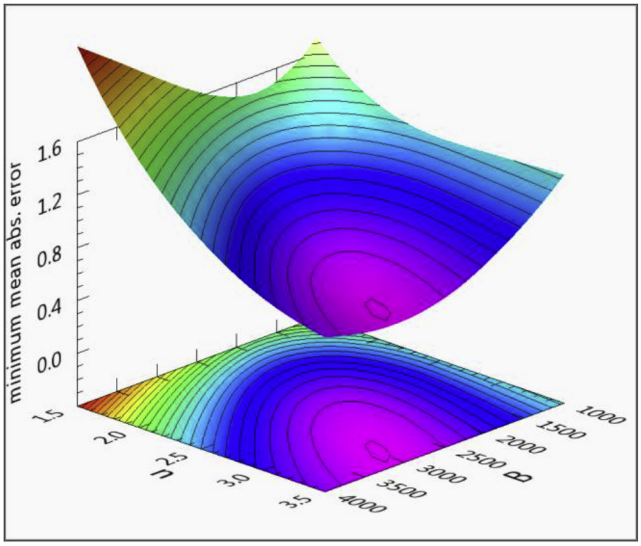

Fig. 4. Surface of the minimum $\varepsilon_{MA,INT}$ as a function of knock integral model parameters *B* and *n* for gasoline.

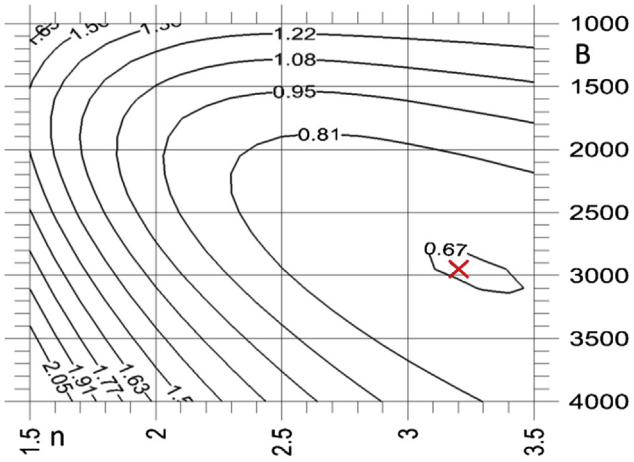

Fig. 5. Contour map of the minimum $\varepsilon_{MA,INT}$ as a function of Knock Integral model parameters B and n for gasoline.

$$\varepsilon_{MA,\ ID} = \frac{\sum_{i=1}^{N} |\varepsilon_{ID,\ i}|}{N} \tag{12}$$

Following the error minimization procedure previously described, the three model parameters corresponding to the minimum error have been determined on the basis of pressure cycles sampled using both gasoline and propane: the results are exposed in Table 6. As can be observed, both ID and KI methods provided similar values of the three model parameters for both fuels, with a comparable level of accuracy in terms of mean absolute error (Tables 5 and 6).

As regards the simultaneous combustion of propane and gasoline, some preliminary considerations have to be pointed out. The results obtained in previous works [1,28,21], as well as the compression ratio needed for causing knocking exposed in Table 3, demonstrates that, as regards knock resistance, the gasoline-air mixture strongly benefits from the addition of propane, even in small quantities; the experimentally observed knock resistance increase can be explained taking into consideration an interaction between the intermediate products of the pre-ignition reactions of both gasoline and propane. During flame front propagation each fuel in the unburned mixture is characterized by a certain number of pre-ignition reactions which are essentially governed by the radicals produced by each single component of the fuel. Due to the very different composition of gasoline (mainly composed by C_4 to C_{12} hydrocarbons [30,31]) and propane (which instead is a C_3), the radicals involved in the chain-branching reactions of gasoline are quite different from those produced by propane, which are characterized by lower reaction rate and longer lives [32,33]. This explains the higher knock resistance of propane (96.7 MON, as reported in Table 4) with respect to gasoline (85 MON). A possible explanation of the knocking resistance increase obtained by adding propane to gasoline may hence be given by supposing that the propane intermediate products interact with gasoline radicals slowing down their reactions and hence the overall auto-ignition process (i.e. increasing the auto-ignition delay time τ). According to the above mentioned considerations, in the simultaneous combustion of propane and gasoline, the auto-ignition process is promoted by the lower knock resistant fuel (gasoline) and slowed down by the higher resistant (propane). Since in both auto-ignition models (Equations (3) and (4)) the two parameters n and B represent the fuel sensitivity to pressure and temperature, for the simultaneous combustion of propane and gasoline the authors considered n and B equal to the values determined for pure gasoline combustion, ascribing only to the parameter A the increased auto-ignition delay due to propane participation; the same procedure has been followed in previous works, such as in [10] for the simultaneous combustion of n-heptane and isooctane and in [13] for the combustion of CNG-gasoline mixtures. Hence, applying the already mentioned minimum search algorithm to the mean absolute error (Equations (11) and (12)) of both KI and ID models using the propane-gasoline mixtures experimental data (Table 2), the authors determined the values of the parameter A for each of the propane mass fraction investigated. Table 7 and Table 8 show the obtained values of the parameter A for the KI and the ID model respectively, together with the corresponding mean absolute and maximum errors.

Table 5
Knock integral model parameters values determined for gasoline and propane.

Fuel	A	n	B	$\varepsilon_{MA,INT}$ [CAD]	$\lvert\varepsilon_{MAX,INT}\rvert$ [CAD]
Gasoline	0.335	3.2	2950	0.67	4.0
Propane	0.0275	3.0	5100	0.58	4.4

Table 6
Ignition delay model parameters values determined for gasoline and propane.

Fuel	A	n	B	$\varepsilon_{MA,ID}$ [CAD]	$\lvert\varepsilon_{MAX,ID}\rvert$ [CAD]
Gasoline	0.360	3.1	2400	0.73	5.1
Propane	0.0130	2.5	4000	0.97	5.8

Table 7
Values of model parameter *A* determined for each propane-gasoline mixture tested (Knock Integral method).

Propane mass fraction (%)	*A*	$\varepsilon_{MA,INT}$ [CAD]	$\lvert\varepsilon_{MAX,INT}\rvert$ [CAD]
0	0.335	0.67	4.0
20	0.555	0.71	3.4
40	0.659	0.78	3.1
60	0.882	0.81	3.6
80	0.990	0.86	3.5

Table 8
Values of model parameter *A* determined for each propane-gasoline mixture tested (ignition delay method).

Propane mass fraction (%)	*A*	$\varepsilon_{MA,ID}$ [CAD]	$\lvert\varepsilon_{MAX,ID}\rvert$ [CAD]
0	0.360	0.73	5.1
20	0.565	0.86	3.5
40	0.675	0.95	3.5
60	0.910	0.97	3.4
80	1.06	1.00	3.6

As can be observed, the two methods provided quite similar results, even though the ID method shows a slightly higher maximum error ($\lvert\varepsilon_{max,ID}\rvert = 5.1$ CAD) with respect to the Knock Integral method (whose maximum error is 4.0 CAD). It is worth to mention that both models provide mean absolute errors always lower than 1 CAD that is an almost negligible quantity from an engine control point of view.

The graph in Fig. 6 reports the progress of *A* obtained by the use of both models, as function of the propane mass fraction.

As can be observed two linear regressions can be drawn, whose equations are here reported:

$$A_{KI}(x_{prop}) = 0.819 \cdot \frac{x_{prop}}{100} + 0.357 \tag{13}$$

$$A_{ID}(x_{prop}) = 0.873 \cdot \frac{x_{prop}}{100} + 0.365 \tag{14}$$

where A_{KI} and A_{ID} refers to KI model and to ID model respectively. This means that the auto-ignition time of a propane-gasoline mixture can be linearly expressed as function of the propane mass fraction. The authors consider this a very interesting property since it allows to evaluate, by simple interpolation, the parameter *A* of the knock prediction models for any propane-gasoline mixtures. However, it must be remarked that the linear regressions in Fig. 6 cannot include the 100% propane because the diagram has been obtained considering the gasoline sensitivity to pressure and temperature, i.e. all the data in Fig. 6 have been obtained maintaining the same values of *n* and *B* determined for pure gasoline.

As far as the knock resistance of the fuel mixture is concerned, a correlation between the parameter *A* and the mixture MON would be very useful, as already stated by other researchers [10]. In a previous work [21] the authors experimentally determined a linear correlation between the gasoline-LPG mixture MON and its LPG molar fraction. Given the high concentration of propane in the LPG used in [21], a similar linear correlation between the MON of propane-gasoline mixture and the propane molar fraction can be assumed. Under this hypothesis, on the basis of MON value and molar mass of the two fuels (110 g/mole for gasoline and 44 g/mole for propane, as detailed in [21]), it is possible to obtain the diagram of Fig. 7, which reports the propane-gasoline mixture MON as a function of the percentage propane mass fraction. Considering the application to engine management, the mass fraction is more suitable than the molar fraction to represent mixture composition since molar fraction is evaluated through the assumed gasoline molar mass, which is affected by a ±10% variability due to composition uncertainty [30,38–40].

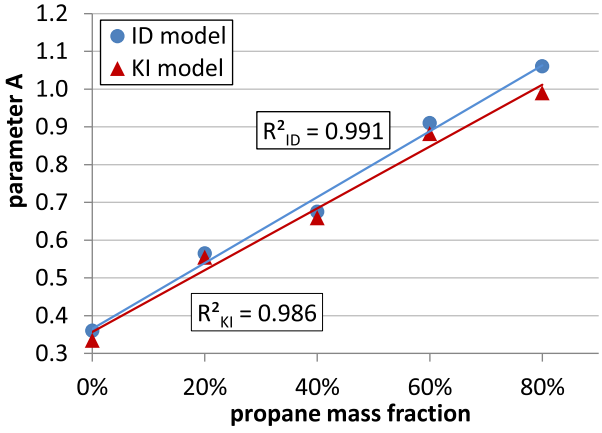

Fig. 6. Model parameter *A* as function of the propane mass fraction.

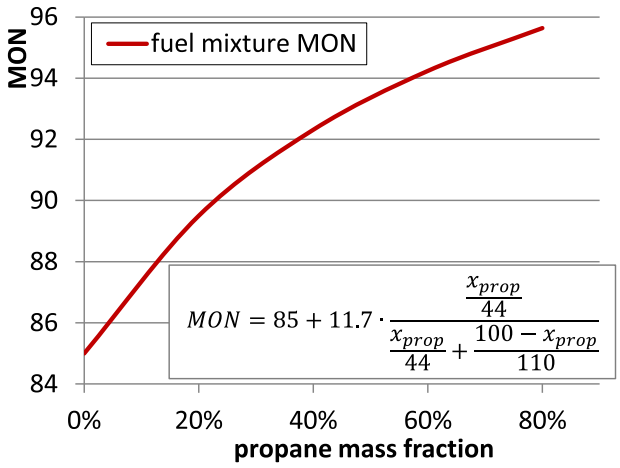

Fig. 7. Fuel mixture MON as function of the propane mass fraction.

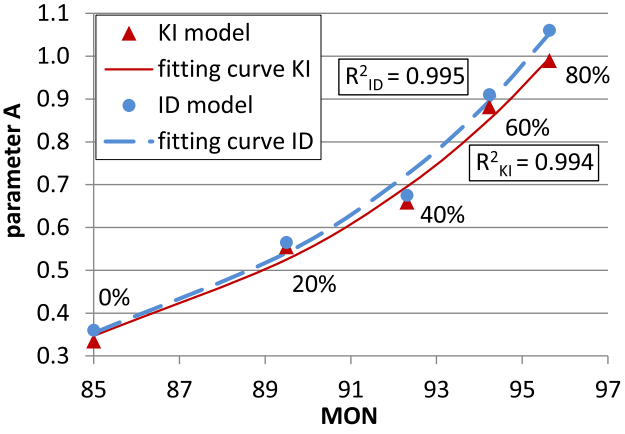

Fig. 8. Model parameter *A* as function of the mixture MON (propane mass fraction is also reported).

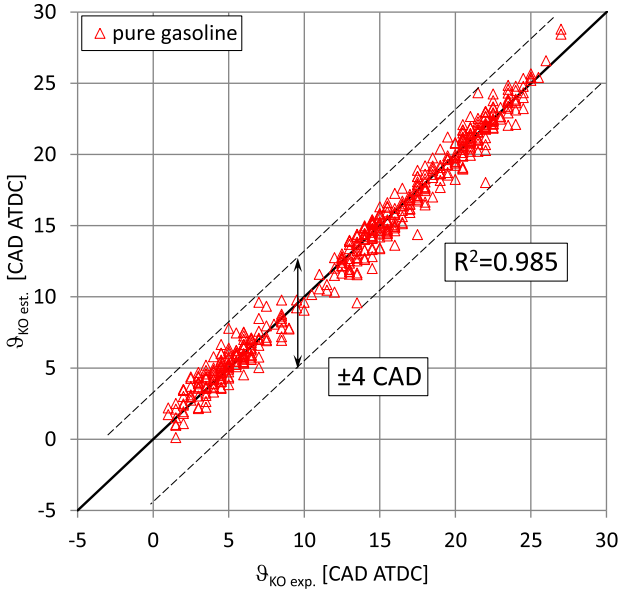

Fig. 9. Comparison between estimated and experimental knock onset crank angles for gasoline (KI method).

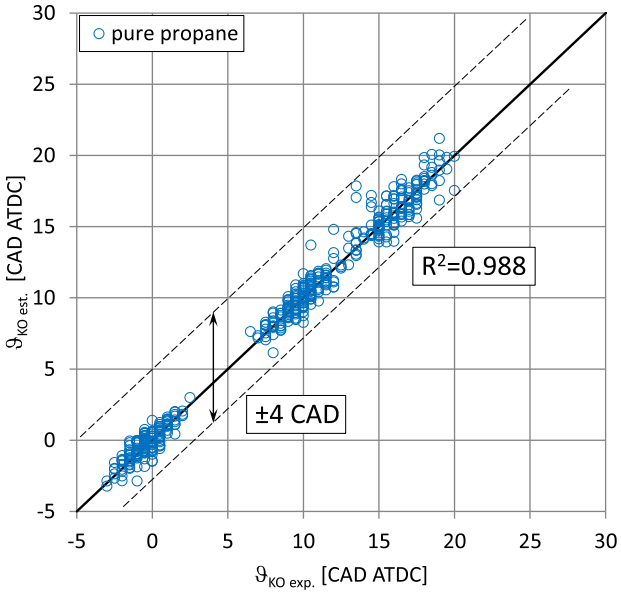

Fig. 10. Comparison between estimated and experimental knock onset crank angles for propane (KI method).

Using the results reported in Figs. 6 and 7 it is possible to trace a correlation between the parameter A and the fuel mixture MON. This correlation is reported in Fig. 8 for both models tested, together with the best fit curves, whose equations are:

$$A_{KI}(MON) = (3.56 - 0.0267 \cdot MON)^{-4.21} \tag{15}$$

$$A_{ID}(MON) = (3.83 - 0.0297 \cdot MON)^{-3.93} \tag{16}$$

In both cases the progress of A shows an increasing slope with the mixture MON, which means a nonlinear correlation between fuel mixture auto-ignition time of Equation (1) and its knock resistance.

After identification, the output of the two models have been compared to experimental data. For each fuel tested: gasoline, propane and their mixtures (i.e. for each set of constants A, n and B), the knock onset position evaluated by each model has been compared with the experimentally measured value. For what concerns the KI model the results of this comparison are shown in Fig. 9 (gasoline), Fig. 10 (propane) and Fig. 11 (propane-gasoline mixtures): as can be observed, a very good correlation is found for all fuels tested with R^2 values ranging from 0.981 (fuel mixtures) to 0.988 (propane); the maximum deviation from the 45° line (i.e. the null error reference) varies from ±3.5 CAD (fuel mixtures) to ±4.0 CAD (gasoline) and the mean absolute errors is between 0.58 CAD (propane) and 0.82 CAD (fuel mixtures).

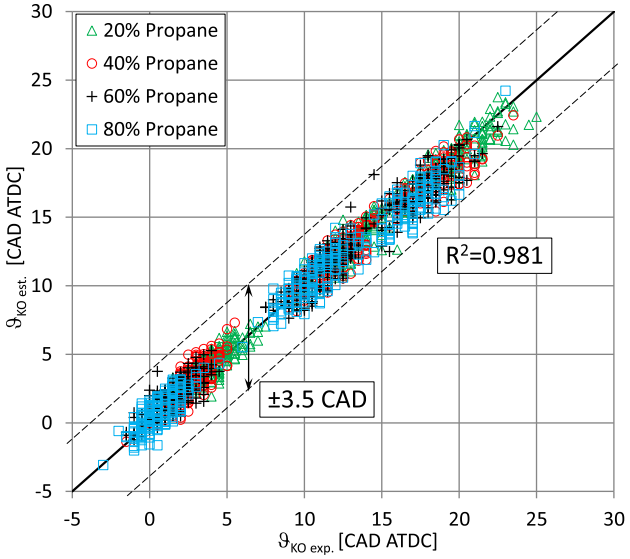

Fig. 11. Comparison between estimated and experimental knock onset crank angles for propane-gasoline mixtures (KI method).

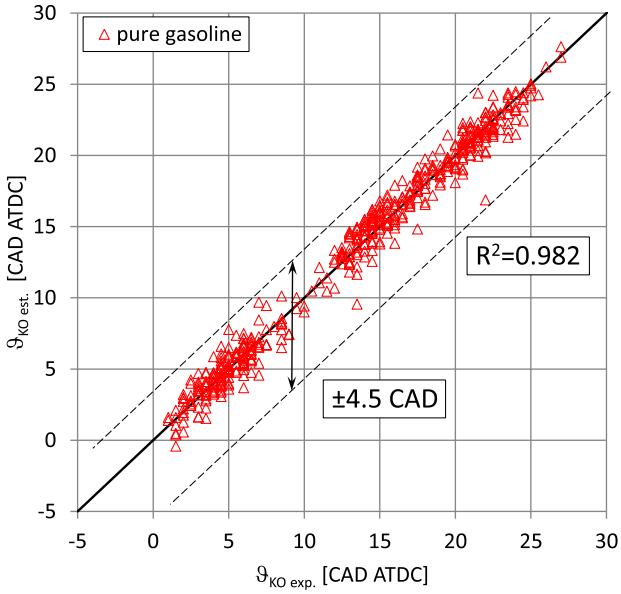

Fig. 12. Comparison between estimated and experimental knock onset crank angles for gasoline (ID method).

These results demonstrate that once properly calibrated, the Knock Integral model is able to predict the knock onset position with a maximum error of about 4 CAD, which is a very satisfactory result, above all if the wide variety of pressure and temperature histories used for model calibration is considered: the experimental data used in effect may represent many different engine geometries and thermodynamic conditions (i.e. different compression ratios and mixture inlet temperatures), and many different fuel compositions (greatly varied within the performed tests, as resumed in Tables 2 and 3).

The same procedure has been followed employing the ID method; the results, reported in Fig. 12 (gasoline), Fig. 13 (propane) and Fig. 14 (propane-gasoline mixtures) show R^2 values ranging from 0.966 (propane) to 0.982 (gasoline), maximum deviations from the 45° line varying from ±3.5 CAD (fuel mixtures) to ±5.0 CAD (propane) and mean absolute errors comprised between 0.96 CAD (fuel mixtures) and 0.97 CAD (propane).

It can be stated hence that the two models employed show a high level of accuracy in terms of both mean absolute error (never higher than 1 CAD) and maximum absolute error (around 4 CAD). In particular, the ID method revealed slightly lower accurate because of its intrinsic simplicity. Since the Knock Integral method is slightly more accurate and requires less computational effort it could be preferred for the implementation in zero dimensional simulations.

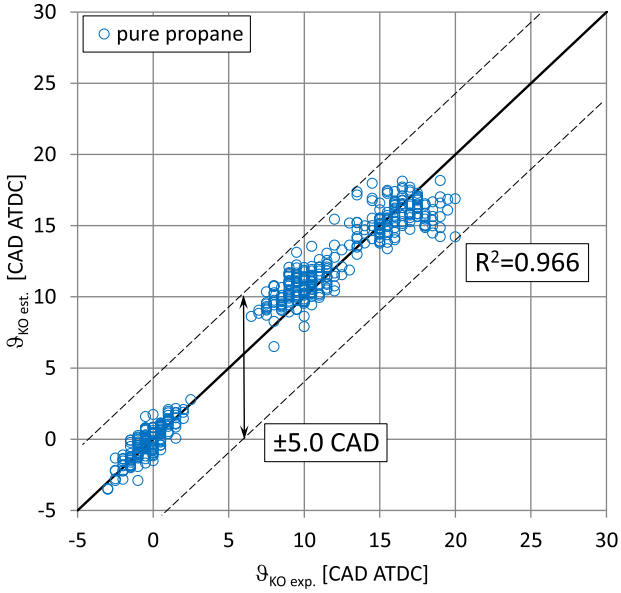

Fig. 13. Comparison between estimated and experimental knock onset crank angles for propane (ID method).

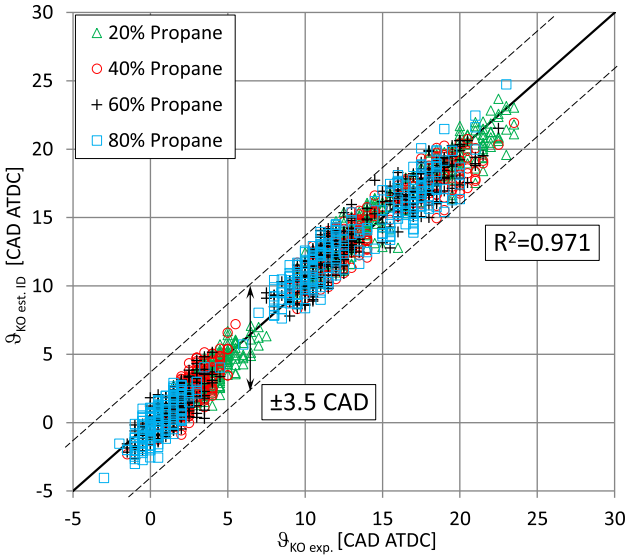

Fig. 14. Comparison between estimated and experimental knock onset crank angles for propane-gasoline mixtures (ID method).

4. Conclusions

The purpose of this work was to provide a reliable knock onset prediction sub-model to be implemented in the usually employed zero dimensional engine thermodynamic simulations, with the aim to allow a knock-safe performance optimization of engines fuelled by propane, gasoline and their mixtures in different proportions. This has been accomplished using two different approach, the Knock Integral method and the Ignition Delay method, whose parameters have been tuned by means of experimental data collected on a properly modified CFR engine. Several light knocking pressure cycles, obtained with a large variation of initial temperature and compression ratio, have been used to obtain reliable knock onset prediction for engines of different kind (naturally aspirated or supercharged) fed by gasoline, propane and their mixtures in every proportions. As shown by experimental results, the auto-ignition time of the propane-gasoline mixtures exhibits a linear trend with respect to propane mass fraction and an increasing slope trend with respect to mixture MON. The present work shows that both models, properly calibrated, accurately predict knock onset with a mean absolute error not higher than 1 CAD which, as already mentioned, is an almost negligible quantity for SI engine management purpose. Due to the slightly lower knock onset errors and to its lower computational effort, the Knock Integral method can be considered preferable for the application in zero dimensional thermodynamic modelling of spark ignition engines.

Symbols and abbreviation

A, B, n	fuel dependent model constants
A_{KI}	a value for knock integral method
A_{ID}	a value for ignition delay method
BTDC	before top dead centre
CAD	crank angle degrees
CFR	cooperative fuel research
CR	compression ratio
E	fuel activation energy
ID	ignition delay
IGBT	insulated gate bipolar transistor
IVC	inlet valve closure
KI	knock integral
KOCA	knock onset crank angle
LPG	liquefied petroleum gas
m	polytropic law coefficient
MAP	manifold absolute pressure
MON	motor octane number
N	total number of pressure cycles acquired for each operative condition
NG	natural gas
PID	proportional integral derivative
p	unburned gas pressure
p_{IGN}	unburned gas pressure at spark ignition

p_{IVC} unburned gas pressure at IVC
p_m experimental mean unburned gas pressure
R universal gas constant
RPM revolutions per minute
SA spark advance
SI spark ignition
t time
T unburned gas temperature
TDC top dead centre
T_{IGN} unburned gas temperature at spark ignition
t_{IVC} inlet valve closure time
T_{IVC} unburned gas temperature at IVC
t_{KO} knock onset time
T_m experimental mean unburned gas temperature
T_{MIX} inlet mixture temperature
V in-cylinder volume
V_{IVC} unburned gas volume at IVC
x_{prop} percentage mass of propane in the total fuel mass of the mixture
ϑ_{IVC} crank angle at inlet valve closure
$\vartheta_{KO,est,\mathrm{INT}}$ KOCA estimated using the integral method
$\vartheta_{KO,est,\mathrm{ID}}$ KOCA estimated using the ID method
$\vartheta_{KO,exp.}$ experimental KOCA
$\varepsilon_{\ \mathrm{INT}}$ integral method KOCA error
$\varepsilon_{\ \mathrm{ID}}$ ID method KOCA error
$\varepsilon_{MA,INT}$ integral model mean absolute error
$\varepsilon_{MA,ID}$ ID model mean absolute error
$\varepsilon_{MAX,INT}$ integral model maximum absolute error
$\varepsilon_{MAX,ID}$ ID model maximum error
τ ignition delay
ω engine angular velocity

References

[1] E. Pipitone, S. Beccari, Performances and Emissions Improvement of an S.I. Engine Fuelled by LPG/Gasoline Mixtures, SAE Technical Paper 2010-01-0615, 2010, http://dx.doi.org/10.4271/2010-01-0615.
[2] E. Pipitone, S. Beccari, Performances Improvement of a S. I. CNG Bi-fuel Engine by Means Double-fuel Injection, SAE Technical Paper 2009-24-0058, 2009, http://dx.doi.org/10.4271/2009-24-0058.
[3] V. Delpech, J. Obiols, D. Soleri, L. Mispreuve, et al., Towards an innovative combination of natural gas and liquid fuel injection in spark ignition engines, SAE Int. J. Fuels Lubr. 3 (2) (2010) 196–209, http://dx.doi.org/10.4271/2010-01-1513.
[4] J. Obiols, D. Soleri, N. Dioc, M. Moreau, Potential of Concomitant Injection of CNG and Gasoline on a 1.6L Gasoline Direct Injection Turbocharged Engine, SAE Technical Paper 2011-01-1995, 2011, http://dx.doi.org/10.4271/2011-01-1995.
[5] M. Momeni Movahed, H. Basirat Tabrizi, M. Mirsalim, Experimental investigation of the concomitant injection of gasoline and CNG in a turbocharged spark ignition engine, Energy Convers. Manag. 11 (February 2014), http://dx.doi.org/10.1016/j.enconman.2014.01.017.
[6] M. Veiga, R. Mansano, R. Silva, C. Gomes, Injection System for Tri-fuel Engines with Control of Power by Simultaneous Use of CNG and Ethanol or Gasoline, SAE Technical Paper 2010-36-0195, 2010, http://dx.doi.org/10.4271/2010-36-0195.
[7] J.C. Linvengood, P.C. Wu, Correlation of autoignition phenomenon in internal combustion engines and rapid compression machines, in: Fifth International Symposium on Combustion, 1955, pp. 347–356, http://dx.doi.org/10.1016/S0082-0784(55)80047-1.
[8] André L. Boehman, Olivier Le Corre, Combustion of syngas in internal combustion engines", Combust. Sci. Technol. 180 (6) (2008) 1193–1206, http://dx.doi.org/10.1080/00102200801963417.
[9] Seref Soylu, Jon Van Gerpen, Development of an autoignition submodel for natural gas engines, Fuel 82 (2003) 1699–1707, http://dx.doi.org/10.1016/S0016-2361(03)00147-9.
[10] Douaud A. M., Eyzat P., "Four-octane-number method for predicting the anti-knock behaviour of fuels and engines", SAE Technical Paper 780080, http://dx.doi.org/10.4271/780080.
[11] Christian Lämmle, Numerical and Experimental Study of Flame Propagation and Knock in a Compressed Natural Gas Engine, Ph.D. thesis presented at the Swiss Federal Institute of technology, Zurich, 2005, http://dx.doi.org/10.3929/ethz-a-005143670.
[12] Wayne W., Clark N., Atkinson C., "Numerical Prediction of Knock in a Bi-fuel Engine", SAE Technical Paper 982533, http://dx.doi.org/10.4271/982533.
[13] E. Pipitone, S. Beccari, Calibration of a knock prediction model for the combustion of gasoline-natural gas mixtures, Pap. No. ICEF2009-14057, in: ASME 2009 Internal Combustion Engine Division Fall Technical Conference, Lucerne, Switzerland, September 27–30, 2009, pp. 191–197, http://dx.doi.org/10.1115/ICEF2009-14057. ISBN: 978-0-7918-4363-5, eISBN: 978-0-7918-3858-7.
[14] Philip Cadman, Geraint O. Thomas, Philip Butler, The auto-ignition of propane at intermediate temperatures and high pressures, Phys. Chem. Chem. Phys. 2 (2000) 5411–5419, http://dx.doi.org/10.1039/B003665J.
[15] B. Radu, G. Martin, R. Chiriac, N. Apostolescu, On the Knock Characteristics of LPG in a Spark Ignition Engine, SAE Technical Paper 2005-01-3773, 2005, http://dx.doi.org/10.4271/2005-01-3773.
[16] Eduard Moses, Alexander L. Yarin, Pinhas Bar-Yoseph, On knocking prediction in spark ignition engines, Combust. Flame 101 (1995) 239–261, http://dx.doi.org/10.1016/0010-2180(94)00202-4.
[17] C.K. Westbrook, W.J. Pitz, Modeling of knock in spark-ignition engines, in: International Symposium COMODIA 90, 1990. OSTI ID: 6755324.
[18] J.B. Heywood, Internal Combustion Engines Fundamentals, McGraw-Hill automotive technology series, 1988, ISBN 0-07-100499-8.
[19] J.I. Ramos, Internal Combustion Engine Modeling, Butterworth-Heinemann Ltd., 1999, ISBN 0750612096.
[20] ASTM Standard D2700, Standard Test Method for Motor Octane Number of Spark Ignition Engine Fuel, ASTM International, West Conshohocken, PA, 2011, http://dx.doi.org/10.1520/D2700.
[21] Pipitone E., Genchi G., "Experimental determination of LPG-gasoline mixtures knock resistance", J. Eng. Gas Turbines power, ASME, http://dx.doi.org/10.1115/1.4027831.
[22] Fairchild Semiconductor Corporation, HGTP14N40F3VL/HGT1S14N40F3VLS Data sheet Rev. B1, February 2002.
[23] Randolph Andrew L., "Methods of Processing Cylinder Pressure Transducer Signals to Maximize Data Accuracy", SAE Paper 900170,http://dx.doi.org/10.4271/900170.
[24] Brunt Michael F. J., Pond Christopher R., "Evaluation of Techniques for Absolute Cylinder Pressure Correction", SAE Paper 970036, http://dx.doi.org/10.4271/970036.

[25] Pipitone E., Beccari A., Beccari S., "Reliable TDC Position Determination: A Comparison of Different Thermodynamic Methods through Experimental Data and Simulations", SAE Paper 2008-36-0059, http://dx.doi.org/10.4271/2008-36-0059.
[26] E. Pipitone, A comparison between combustion phase indicators for optimal spark timing, J. Eng. Gas Turbines Power ASME 130 (5) (Jun 19 2008), http://dx.doi.org/10.1115/1.2939012.
[27] J.A. Nelder, R. Mead, A simplex method for function minimization, Comput. J. 7 (1965) 308–313, http://dx.doi.org/10.1093/comjnl/7.4.308.
[28] G. Genchi, E. Pipitone, S. Beccari, A. Piacentino, Knock Resistance Increase through the Addition of Natural Gas or LPG to Gasoline: An Experimental Study, SAE Technical Paper 2013-24-0100, 2013, http://dx.doi.org/10.4271/2013-24-0100.
[29] Bob Boundy, Susan W. Diegel, Lynn Wright, Stacy C. Davis, Biomass Energy Data Book, fourth ed., U. S. Dep. Of Energy, 2011. ORNL/TM-2011/446, http://cta.ornl.gov/bedb/download.shtml.
[30] American Petroleum Institute (API), Alcohols and Ethers, Publication No. 4261, second ed., July 1988. Washington DC.
[31] N. Nikolaou, C.E. Papadopoulos, I.A. Gaglias, K.G. Pitarakis, A new non-linear calculation method of isomerisation gasoline research octane number based on gas chromatographic data, Fuel 83 (4–5) (March 2004) 517–523. http://dx.doi.org/10.1016/j.fuel.2003.09.011.
[32] Goutham Kukkadapu, Kamal Kumar, Chih-Jen Sung, Marco Mehl, William J. Pitz, Experimental and surrogate modeling study of gasoline ignition in a rapid compression machine, Combust. Flame 159 (10) (October 2012) 3066–3078. http://dx.doi.org/10.1016/j.combustflame.2012.05.008.
[33] Juan C. Prince, Forman A. Williams, Short chemical-kinetic mechanisms for low-temperature ignition of propane and ethane, Combust. Flame 159 (7) (July 2012) 2336–2344. http://dx.doi.org/10.1016/j.combustflame.2012.02.012.
[34] Kai J. Morganti, Tien Mun Foong, Michael J. Brear, Gabriel da Silva, Yi Yang, Frederick L. Dryer, The research and motor octane numbers of liquefied petroleum gas (LPG), Fuel 108 (June 2013) 797–811. http://dx.doi.org/10.1016/j.fuel.2013.01.072.
[38] J.E. Anderson, D.M. DiCicco, J.M. Ginder, U. Kramer, T.G. Leone, H.E. Raney-Pablo, T.J. Wallington, High octane number ethanol-gasoline blends: quantifying the potential benefits in the United States, Fuel 97 (July 2012) 585–594. http://dx.doi.org/10.1016/j.fuel.2012.03.017.
[39] J.E. Anderson, U. Kramer, S.A. Mueller, T.J. Wallington, Octane numbers of ethanol-and methanol-gasoline blends estimated from molar concentrations, Energy Fuels 24 (12) (2010) 6576–6585, http://dx.doi.org/10.1021/ef101125c.
[40] Ashish S. Lanje, M.J. Deshmukh, Performance and emission characteristics of SI engine using LPG-ethanol: a review, Int. J.Emerg. technol. Adv. Eng. 2 (10) (October 2012) 2250–2459.